21st International Conference on
Harmonisation within Atmospheric Dispersion Modelling for Regulatory Purposes
27-30 September 2022, Aveiro, Portugal

IMPACTS OF AN EVAPORATING WATERBODY IN URBAN FABRIC THROUGH CFD SIMULATIONS

Carlo Cintolesi[1], Petros Ampatzidis[2], Andrea Petronio[3] and Silvana Di Sabatino [1]

[1]Department of Physics and Astronomy, University of Bologna, Bologna, Italy
[2]Department of Architecture and Civil Engineering, University of Bath, Bath, UK
[3]IE-FLUIDS s.r.l, Trieste, Italy

Abstract:
The evaporation and condensation of water are crucial phenomena that drives many physical processes in urban environment both in terms of buoyancy force generated and heat sink or source introduced. This work presents and implements a general evaporation and condensation model that includes the heat exchange due to the water change of phase. Such a general approach can be applied to different simulation techniques link RANS and LES. Two geometries paradigmatic of a city fabric are investigate under a mixed convective regime and considering waterbodies which are set to be warmer and colder compared to the building temperature. Globally, the water evaporation leads to an increase of convective motions that enhance the vertical transport and the turbulent mixing between urban canyons and the surrounding atmosphere. To the best of the authors knowledge, this is one of the first study directly reproducing the evaporation form a waterbody in urban context.

Key words: *Urban Canyon, Water Evaporation, Computational Fluid Dynamics, OpenFOAM.*

INTRODUCTION

Nowadays, critical issues affect the human health and the liveability in city contexts, including the Urban Heat Island and Urban Pollutant Island, which are expected to be exacerbated by the actual trend of climate change. To address such issues, there is a growing interest in Nature-Based Solutions (NBSs) as tools to develop suitable mitigation and adaptation strategies (EC, 2015). Nonetheless, there is no clear consensus on the efficacy and best practices to implement NBSs, that can exhibit benefits as well as unexpected collateral effects. The present contribution wants to address this lack by analysing the impact of blue NBSs, such as waterbodies, on the thermo-fluid dynamics of two archetypal urban configurations. Overall, the water evaporation reduces the temperature within urban canyons, while increasing the convection and turbulent mixing at the roof-top level; thus, enhancing the mass and momentum exchange between the canyon and surrounding atmosphere. The physical process is numerically reproduced utilising two computational fluid dynamics techniques: the Large-Eddy Simulations (LES) that directly reproduces a large part of turbulence fluctuations, and the Reynolds-Averaged Navier-Stokes (RANS) simulations which allows for studying complex geometries thanks to the low computational cost. The thin water film model is adopted to account for the water change of phase and the consequent heat transfer (Cintolesi et al, 2016 & 2017). Such model is implemented in new solvers, developed within the OpenFOAM (2018) toolbox. Two configurations have been investigated: (i) an idealised urban canyon is studied in detail through LES, showing that a waterbody is particularly effective in improving the in-canyon circulation, turbulent kinetic energy and turbulent kinetic fluxes at the roof-top interface; (ii) a more realistic configuration reproducing an array of 7×3 square building with a waterbody in the middle is simulated and analyses through RANS. In the following, we provide a brief overview of the implemented mathematical model with references for further details and a complete description, an outlook of the two cases under analysis with the main results, and some final comments.

MATHEMATICAL MODEL AND SIMULATION APPROACH

The mathematical model for the air dynamics and for the water evaporation, as well as the simulation approaches adopted, are here shortly reported. A complete discussion and description of the models can be found in the reported references. Simulations have been performed using the open-source software

OpenFOAM (2018), using a home-made solver implementing the evaporation model. All the simulations have been successfully validated against experimental and numerical datasets reported in literature.

Governing equations

The air is considered an incompressible fluid and the Boussinesq approximation is adopted for the buoyancy effects. The governing equations read:

$$\frac{\partial u_j}{\partial x_j} = 0, \tag{1}$$

$$\frac{\partial u_i}{\partial t} + u_j \frac{\partial u_i}{\partial x_j} = -\frac{\partial p}{dx_i} + \nu \frac{\partial^2 u_i}{\partial x_j \partial x_j} + b_i, \tag{2}$$

$$b_i = g_i(1 - \beta_T \Delta T - \beta_\omega \Delta\omega), \tag{3}$$

where u_i is the air velocity component, p is pressure,ν in the kinematic viscosity, and $b_i$is the buoyancy force. This last is the sum of the temperature and vapour contribution: $g_i$is the gravity acceleration vector, $\beta_{T/\omega}$is the thermal/vapour expansion coefficient, ΔT and $\Delta\omega$ are the variation of temperature and vapour concentration (respectively) with respect to the reference temperature and vapour. Equations for temperature and vapour concentration are:

$$\frac{\partial T}{\partial t} + u_j \frac{\partial T}{\partial x_j} = \alpha_T \frac{\partial^2 T}{\partial x_j \partial x_j} + S_\omega, \tag{4}$$

$$\frac{\partial \omega}{\partial t} + u_j \frac{\partial \omega}{\partial x_j} = \alpha_\omega \frac{\partial^2 \omega}{\partial x_j \partial x_j}, \tag{5}$$

where $\alpha_{T/\omega}$is the thermal/vapour molecular diffusivity and S_ω is the sink term due to the evaporation of water at the boundary of the air domain.

The water model is based on the thin-film assumption, i.e. the waterbody is modelled as a wet surface that can evaporate infinitely (Petronio, 2010). The velocity of evaporation U_ω essentially depends on the vapour gradient in the surface normal direction, and it is estimated with a semi-impermeable model (Welty et al., 2007), that reads:

$$U_{\omega,i} = -\frac{\alpha_\omega}{1-\omega_\Gamma}\left(\frac{d\omega}{dn_i}\|_\Gamma\right) n_i, \tag{6}$$

with n_i the normal versor to the wet surface. The subscript Γ denotes that quantities are evaluated at the surface; hence, the evaporation velocity is defined just at the wet surface. The heat sink S_ω is proportional to the divergence of the evaporation velocity as follows:

$$S_\omega = \frac{1}{\rho\, C_p}\frac{\partial}{\partial x_i}\left(\rho_\star L_h U_{\omega,i}\right), \tag{7}$$

where ρC_p are the density and specific heat of air, respectively, while $\rho_\star$ is the density of the mixture of air and water vapour, which is taken equal to air density for simplicity, and L_h is the latent heat of vaporization. The temperature sink term is numerically applied to the first cell near the wet surface in the air domain. Additional information and a complete description of the present evaporation model can be found in Cintolesi et al. (2016, 2017).

WATER CHANNEL IN AN IDELISED URBAN CANYON

The first case study (see Figure 1) consists of an infinite array of urban canyons with a unity aspect ratio, including a water channel at the street level ($0.65 < x/H < 1.35$). This case was simulated with the Large-Eddy Simulation technique (e.g. Sagaut, 2000), using the Smagorinsky (1963) model to account for the unresolved Sub-Grid Scale (SGS) turbulent motions. The atmospheric wind leads to a Reynolds

number based on the free-stream velocity U_0 is $Re = U_0 H/\nu = 2 \times 10^4$; hence, within the range of the Reynolds independence. Temperature of the buildings and domain is constant while different temperatures are imposed on water. The domain is discretised using 1,592,562 cells and the mesh is stretched near the solid and water surfaces ensuring a direct resolution of the wall-boundary layer. The numerical schemes used for solving the equations ensure an overall accuracy of the second order. The simulations are run until a steady-state statistical regime is established, and then the statistics are collected for analysis. Details on geometry, mesh and numerical settings can be found in Cintolesi et al. (2021). Three configurations are studied: the neutral case without channel (as a reference), the warmer case where the channel is hotter than buildings (Richardson number $Ri = 3.4$), and the colder case where the channel is colder than buildings ($Ri = -3.4$). The Richardson number indicates that both cases are in free convection regime; notice that the positive and negative signs are introduced to distinguish the cases with hot and cold water, respectively.

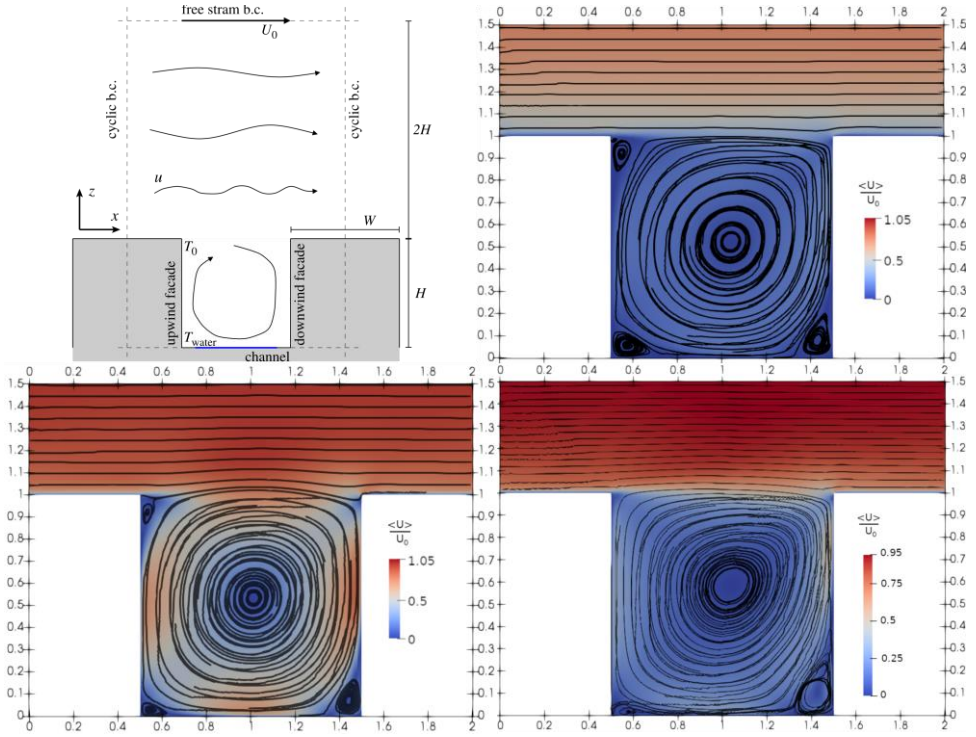

Figure 1. From the top-left panel in clockwise order: geometry of idealised urban canyon; streamwise dimensionless velocity distribution and streamlines for neutral case (no waterbody); the warmer waterbody; the colder waterbody.

Figure 1 shows the dimensionless streamwise velocity intensity and the streamlines in the canyon for the three cases under consideration. Compared to the neutral case (top-right panel), the warmer channel (bottom-left panel) exhibits an increased in-canyon circulation, less extended corner-recirculation regions, and higher out-canyon velocity. The colder channel (bottom-right panel) slightly increases the in-canyon motion while increasing the out-canyon flow velocity and destroys the corner-recirculation regions at the upwind façade. This is mainly due to the vertical velocity generated at this façade by the buoyancy force triggered by the cold air advected from the channel. The increase in velocity above the canyon is probably due to the destruction of the roof shear layer by the vertical motions generated by the buoyancy. The temperature and vapour fields (not shown) are essentially higher in a thin layer near the water channel, while they are rather homogenously distributed inside the canyon. Outside the canyon they tend to rapidly assume their reference values. In both cases, the temperature in the canyon drops due to the evaporation process, which produces an energy sink at the surface of the water. In the case of the warmer channel, this sink is counterbalanced by thermal conduction, the temperature drop is of the order of 3% inside the canyon, and imperceptible outside. In the case of the colder channel, the cooling is much more intense: between 10-20% in the canyon and about 7% outside. Second-order statistics (not here reported) show a general increase in turbulent kinetic energy: overall, with four times in the warmest case, three times in the coldest case compared to the neutral one, and especially at the roof level of buildings where turbulent

exchanges with the atmosphere are most intense. Mean turbulent kinematic momentum fluxes $u'w'/u_0^2$ exhibit larger peaks at height $z/H = 1$, indicating a region of greater mixing at vertical turbulent transport.

WATERBODY IN A SIMPLIFIED URBAN NEIGBORHOOD

The second case study (see Figure 2) consists of a simplified urban neighbourhood composed of a grid of 7×3 square buildings, where the central building has been replaced by a square waterbody placed in the centre of a square. This case was investigated through a RANS simulation, utilizing the RNG $k-\varepsilon$ turbulence model. A synthetic turbulent atmospheric boundary layer impacts the buildings along the x-direction giving a Reynolds number of $Re = 2.9 \times 10^4$. The computational grid counts 846,976 cells and wall functions are used to correctly reproduce the wall-boundary layer. Details of the validation, computational grid and settings can be found in Ampatzidis et al. (2022). Three cases are simulated: neutral (no waterbody), warmer waterbody with respect to the building constant temperature ($Ri = 1.1$), and colder waterbody ($Ri = -1.1$). Again, the flow regime is of mixed convection.

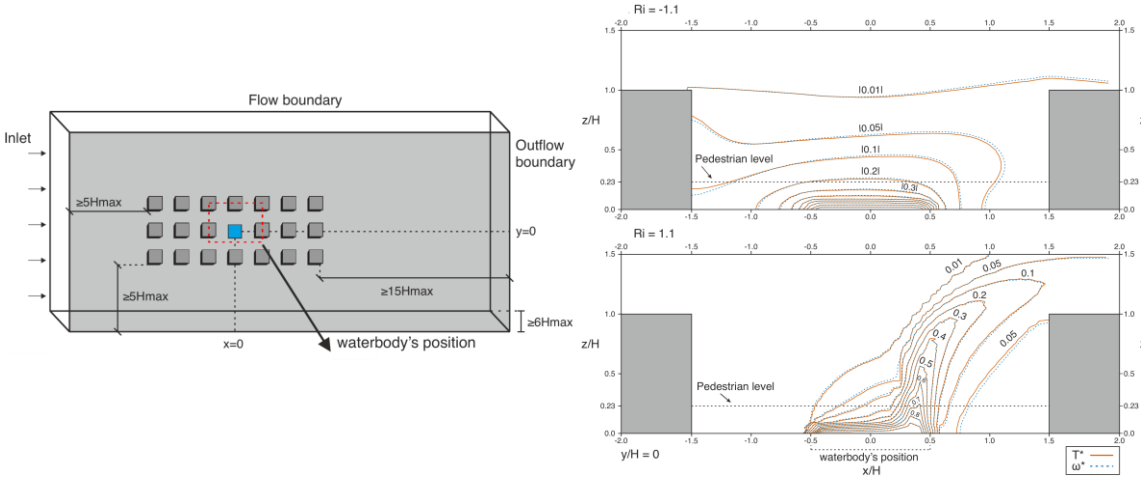

Figure 2. Vertical section along the x-direction of the waterbody square. Left panel: geometry and computational domain. Right panel: dimensionless temperature and vapour contour lines above the waterbody for colder case (top) and warmer case (bottom).

Figure 2 shows the contour line of the dimensionless temperature $T^* = (T - T_0)/\Delta T$ and vapour concentration $\omega^* = (\omega - \omega_0)/\Delta\omega$ in the square with waterbody. Temperature and vapour present similar features and in both cases (colder and warmer waterbody) and higher concentrations are localised in a thin layer above the water surface. However, the colder case exhibits an increase of thermo-vapour stratification and a moderate reduction of temperature in the square, while the warmer case develops a strong upward thermal-vapour plume which drives above the buildings the hot and humid air. The air circulation (not shown) in the square presents a large clockwise vortex, which is reduced by extension and intensity in the colder case and is destroyed by the upward thermal plume in the warmer case. Turbulent kinetic energy peaks near the top corner of the downwind building for the neutral and colder case, while the warmer case has a spot of high turbulent energy where the upward plume is deviated by the ambient airflow (Ampatzidis et al., 2022). Between the downwind building, the circulation is not significantly altered in the colder case and shows a regime similar to the skimming flow, where the in-building circulation is dominated by the main recirculation vortex. On the contrary, in the warmer case, the recirculation region is destroyed, and the in-building flow is no longer separated from the surrounding atmospheric wind.

FINAL REMARKS

A water evaporation model that accounts for heat transfer by the water change of phase has been applied for numerical simulations of two archetypal cases: an idealised urban canyon with water channel and a

simplified urban neighbourhood with a waterbody in a square, and in a regime of mixed convection. The former is reproduced by a high-accurate LES, the latter by a RANS simulation. For both geometries, three scenarios are investigated: the neutral case (no waterbody) is compared with the case including a warmer and a colder waterbody (compared to the building constant temperature). In the idealised urban canyon, the warmer channel triggers a thermo-vapour buoyancy force that enhances the main clockwise vortex, at the same time the in-canyon temperature does not increase because of the cooling effect of the evaporation. The colder channel does not improve the internal vortex velocity (but a localised buoyancy force generated near the upwind buildings remove the corner recirculation regions) and reduce the temperature in the canyon. In both cases, the presence of vertical convective motions increases the turbulence intensity and turbulent kinetic fluxes at the building-roof level, leading to a larger mass and momentum exchange between the canyon and the surrounding atmospheric wind. In the simplified urban neighbourhood, overall, the presence of waterbody promotes mixing and increased the circulation in the square and downwind between buildings. The colder waterbody increases the thermo-vapour stratification in the square and slightly alter the air dynamics, while the warmer waterbody generates a strong upward convective plume that destroy the recirculation vortex in the square and the skimming flow regime in the downwind building canyons. The warmer case can represent a night-time configuration in real city, when the waterbody heated during the day can improve mixing and vertical flows (thus also the dispersion of pollutants). Overall, waterbodies generate vertical convective motions which help removing air from the canyons, increase the turbulent vertical transport and mixing, and overall reduce temperature within the canyons. As a possible side effect, blue infrastructures in city context can lead to an increase in humidity, which can decrease environmental comfort. These are early works under simplifying assumptions (e.g. thermally neutral atmosphere) and further work is needed to expand the study. blue infrastructure in city context which are composed also by these positive effects should be balanced by an increase in humidity, which can decrease environmental comfort.

REFERENCES

Ampatzidis P., C. Cintolesi, A. Petronio, S. Di Sabatino, T. Kershaw, 2022: Evaporating waterbody effects in a simplified urban neighbourhood: a RANS analysis. *Accepted for publication on J. of Wind Engineering and Ind. Aerodynamics*.

Cintolesi, C, A. Petronio, V. Armenio, 2016: Large-eddy simulation of thin film evaporation and condensation from a hot plate in enclosure: First order statistics, *Int. J. of Heat and Mass Transfer*, **101**.

Cintolesi, C, A. Petronio, V. Armenio, 2017: Large-eddy simulation of thin film evaporation and condensation from a hot plate in enclosure: Second order statistics, *Int. J. of Heat and Mass Transfer*, **115**.

Cintolesi C., F. Barbano, S. Di Sabatino, 2021: Large-eddy simulation analyses of heated urban canyon facades, *Energies*, **14**.

EC - European Commission, 2015: Nature-Based Solutions and Re-Naturing Cities, Final Report of the Horizon 2020 Expert Group on Nature-Based Solutions and Re-Naturing Cities, European Union, Brussels.

OpenFOAM, 2018: The OpenFOAM Foundation, version 6.0. Available online: openfoam.org (accessed on 1 May 2019).

Petronio, A., 2010: Numerical investigation of condensation and evaporation effects inside a tub. Ph.D. thesis. School of Environmental and Industrial Fluid Mechanics, University of Trieste.

Sagaut, P., 2000: Large eddy simulation for incompressible flows: an introduction. Springer, Berlin

Smagorinsky, J., 1963: General circulation experiments with the primitive equations: I: the basic experiment. *Mon Weather Rev* 91-99

Welty, J., C. Wicks, G. Rorrer, R. Wilson, 2007: Fundamentals of Momentum, Heat and Mass Transfer. Wiley.